Acta Tropica 215 (2021) 105805

Contents lists available at ScienceDirect

Acta Tropica

journal homepage: www.elsevier.com/locate/actatropica

Influence of gamma radiation on Amphotericin B incorporated in PVP hydrogel as an alternative treatment for cutaneous leishmaniosis

Maria José Alves de Oliveira [a,*], Gethzemani Mayeli Estrada Villegas [b], Flávia Daniela Motta [c], Omar Fabela-Sánchez [d], Arián Espinosa-Roa [b], Wesley Luzetti Fotoran [e], Janaína Capelli Peixoto [e], Fabia Tomie Tano [e], Ademar Benévolo Lugão [a], Pablo Antonio Salvador Vásquez [a]

[a] Nuclear and Energy Research Institute-IPEN-CNEN/SP, Av. Professor Lineu Prestes, 2242, - Cidade Universitária CEP 05508-000, São Paulo-SP, Brazil
[b] CONACyT–Centro de Investigación en Química Aplicada, Av. Alianza Sur 204 Parque de Innovación e Investigación Tecnológica, Apodaca, Nuevo León, 66629 México
[c] Faculdades Oswaldo Cruz Rua Brigadeiro Galvão, n° 540 - Barra Funda CEP, 01151-000, São Paulo-SP, Brazil
[d] CONACyT–Centro de Investigación en Química Aplicada, Blvd. Enrique Reyna 140, Col, San José de los Cerritos, 25294, Saltillo, Coahuila, México
[e] Departamento de Parasitologia, Universidade de São Paulo, Av. Professor Lineu Prestes, Cidade Universitária, 05508-000, São Paulo-SP, Brazil

ARTICLE INFO

Keywords:
Amphotericin B
Leishmaniasis
Gamma irradiation
Hydrogel
Delivery drug

ABSTRACT

Amphotericin B (Amph-B) is an antifungal drug used intravenously for the treatment of leishmaniasis. Side-effects from Amph-B treatment can arise such as cardiac arrhythmia and renal dysfunctions, which will lead to discontinuation of treatment. Unfortunately, patients in endemic countries do not have access to alternative therapies. The objective of this study was to analyze the effects of Cobalt-60 gamma irradiation on crosslinking polymeric hydrogels (Hydg) and the incorporation of Amph-B into the gel as a controlled-release drug delivery alternative. Polyvinylpyrrolidone (PVP)/Amph-B solutions were irradiated with 15 kGy at 0 °C and 25 °C. The drug's stability was ascertained by UV–visible spectrometry, liquid chromatography/mass spectrometry and proton nuclear magnetic resonance. Irradiated Hydg/Amph-B achieved similar stability to the standard Amph-B solution and was enough to promote hydrogel crosslinking. *In vitro* trials were carried out to ensure Amph-B was still biologically active after irradiation. The results from flow cytometry and MTT assay show that Amph-B had an $IC_{50} = 16.7$ nM. A combination of Hydg at 1.324 gmL^{-1} and Amph-B at 25.1 nM for 24 h lead to the greatest inhibition of L. *amazonensis* promastigotes, and could be used as an alternative treatment method for cutaneous leishmaniosis.

1. Introduction

The controlled-release drug delivery system offers a major advantage for drug administration (Buenger et al., 2012; Demeter et al., 2017). Direct drug delivery into the wound diminishes toxicity engendered by conventional administration systems (Aqil et al., 2005; Yano et al., 2002). For each drug, the individual therapeutic range has been determined and correlates with a dose-dependent plasma level. This provides optimal therapy without unacceptable side-effects (Tamargo et al., 2015). Occasionally, certain drugs have a narrow therapeutic window, as is the case for antimoniates and Amphotericin B (Amph-B) in the treatment of leishmaniasis (Oliveira et al., 2016; Lee et al., 2001). Antimoniates, as an injectable form are the primary treatment choice for leishmaniasis and include antimonials, sodium stibogluconate, and meglumine antimoniate (Borborema et al., 2005). When there is a lack of response to these drugs, Amph-B is used as a second-line medication and similarly only exists as an injectable form (Wortmann et al., 2010). Amph-B is a polyene drug used to treat severe fungal infections and is administered as a deoxycholate-solubilized free drug (Murphy et al., 2010). However, there is a decrease in the use of Amph-B due to a major limitation imposed by a close drug-toxicity dose (Al-Mohammed et al., 2005). Several unwanted side-effects have been observed by Amph-B and include arrhythmia and renal dysfunctions. If patients present with any side-effect they will be unable to continue their treatment. This presents a problem to endemic countries where Leishmaniasis is still a growing problem and the range of available medications is relatively

* Corresponding author.
E-mail address: mariajhho@gmail.com (M.J.A. Oliveira).

https://doi.org/10.1016/j.actatropica.2020.105805
Received 14 July 2020; Received in revised form 2 December 2020; Accepted 21 December 2020
Available online 30 December 2020

limited (Amato et al., 2007). Therefore most patients will be unable to access further treatment.

Several attempts have been made to immobilize monomers or dimers of Amph-B using nanostructures combined with polysaccharides, polypeptides, dendrimers, silica nanoparticles, and carbon nanotubes to treat fungal infections (Tutaj et al., 2016; Shu et al., 2018; Ruiz et al., 2014; Chávez-Fumagalli et al., 2015). In light of the aforementioned, new administration proposals have been made to use polymer hydrogels as a matrix for the release of drugs in the treatment of cutaneous wounds (Sumit Mishra et al., 2018; Sosa et al., 2019). Once released, the drug spreads directly into the wound tissue (Bhattarai et al., 2010). This method is used to generate both diffusion and capture systems (Dash et al., 2011). Hydrogels are crosslinked polymer chains generated from either chemical, physical (freezing thermal cycling), or ionizing radiation. Therefore, some polymer chain solutions subjected to gamma (γ) irradiation can become susceptible and form radicals. These radicals recombine to form a three-dimensional network which is a characteristic of hydrogels (Henke et al., 2005). This method is a highly versatile and simple way to obtain hydrogels that are composed of 75 - 85% water (Holback et al., 2011). If subjected to conditions which promote swelling, the hydrogel expands to a volume $\leq$ 300% its original size in water or biological fluids, without structural damage and without modifying its physicochemical characteristics. Therefore, ionizing radiation generated from a cobalt-60 source promotes crosslinking in hydrogels without the need of further additives (chemical catalysts) and produces a ready to use product (Khampieng et al., 2014; Abad, 2016). This method is a suitable tool for the synthesis of hydrogels for biomedical applications.

Indeed, ionizing radiation from either high-energy irradiation or γ ray sources needed for sterilization can generate chemical reactions that lead to undesirable changes to the physicochemical properties of some drugs. This decreases the therapeutic activity of some bioactive molecules and can sometimes form highly toxic species. In contrast, some studies have shown that sterilization by γ irradiation was safe for certain drug delivery systems, such as implantable delivery rods with Fluconazole (FLU) loaded in poly D,L-lactic acid (PLA) and poly L-lactic acid (L-PLA). FLU delivery rods had unaffected loading efficiency, chemical stability, and maintained its crystallographic structure (Soriano et al., 2006). Additionally, some antibiotics such as amoxicillin and cefaclor are radioresistant and can be sterilized with an irradiating dose of 25 kGy without any detrimental effect on their chemical properties or antibacterial activity (Krause et al., 1982). The objective of this study was to analyze γ irradiation effects on Amph-B to use the γ crosslinked hydrogel as an alternative treatment for cutaneous leishmaniasis. The *in vitro* leishmanicidal activity of Amph-B was only validated in promastigote forms of *Leishmania amazonensis (*L. *amazonensis)*, PH8 strain. We show that such Amph-B-loaded hydrogels might be an option for *in situ* therapy, by preventing side effects caused by systemic application and maintaining Amph-B's antiparasitic properties and structure even after irradiation treatment.

2. Materials and methods

2.1. Irradiation of Amph-B

To evaluate the stability of Amph-B (molecular formula: $C_{47}H_{73}NO_{17}$ and molecular mass: 924.07 g/mol) when exposed to γ irradiation, a control solution of Amph-B solubilized with the excipient sodium deoxycholate (molecular mass: 392.00 g/mol, Cristalia) was prepared and then further divided into two groups. They were then placed separately into Styrofoam boxes at different temperatures (0 °C and 25 °C) and irradiated at a rate of 15 kGy/h in a multipurpose cobalt-60 irradiator at the Radiation Technology Center (CETER) in the Nuclear and Energy Research Institute (IPEN), Brazil. To easily distinguish between irradiated and non-irradiated Amph-B samples we referred to them as Amph-B and I/Amph-B, respectively

2.2. Characterization and stability of Amph-B after irradiation

UV-visible spectroscopy was adopted for comparing qualitative Amph-B and I/Amph-B peaks in the 300–500 nm range using the Molecular Devices SpectroMax® i3, at the Biomaterial's laboratory in IPEN. The equipment used for the HPLC Controller was as follows: CBM-20A, pumps: LC-20AD, detector: SPD-20A, oven: CTO-20A, self-injector: SIL 20AC and were obtained from Shimadzu. The conditions used were H_2O, 0.1% formic acid, and acetonitrile. The column used was the Phenomenex Luna C18 (250 × 4.6 mm; 5 μm), time oven: 40 °C, and flow rate: 1.0 $mLmin^{-1}$. The mass spectrometer (MS) (AmaZon Speed ETD [Bruker]) nebulizer: 27 Psi, dry gas: 12 $mLmin^{-1}$, temp: 300 °C, HV: 4500 V. The Analytical centre (Chemistry Institute, University of São Paulo, Brazil) evaluated the molecular stability of the drug after irradiation. Nuclear magnetic resonance (NMR) spectroscopy was used to compare the peaks of Amph-B and I/Amph-B, to analyze the degradation caused by ionizing radiation from Cobalt-60 (Avance™ III HD, [Bruker]) 500 MHz, PROBHD 5 mm PATXI 1H / PULPROG zg30 and MeOD as a solvent.

2.3. Hydg/Amph-B hydrogel synthesis

Synthesis of the hydrogel membrane required preparation of a solution of 8% PVP (molecular weight: 360 000 g/mol (Êxodo), 1% agar (Synth), 1.5% Polyethylene glycol (PEG 400, molecular weight: 380–420 g/mol, (Synth), and 1.5% Laponite RD clay (Colomix) in pure water. After the endothermic solubilization, the formula was cooled to 40 °C and 15 mg of Amph-B / sodium deoxycholate excipient was added. A 2 mm layer formulation was placed in a polyvinyl chloride (PVC) mold (8.0 cm x 13.5 cm x 2 cm), which was sealed and then subjected to γ irradiation from a cobalt-60 source at 15 kGy dose (5.0 ratio of kGy/h) at 25 °C to simultaneous crosslink and sterilize.

2.4. Cultivation of L. amazonensis promastigotes (PH8)

The culture was performed after animal extraction in axenic culture. L. *amazonensis* promastigotes (IFLA/BR/67/pH8) passage 9, were cultivated in M199 medium (Sigma-Aldrich) supplemented with 10% inactivated fetal bovine serum (Gibco/Invitrogen). Promastigotes strain pH8 were cultivated in M199 medium (Sigma-Aldrich, supplemented with 40 mM HEPES pH 7.4, 0.1 mM adenine, 0.005% of hemin, 10% inactivated fetal bovine serum (Gibco/Invitrogen), and 0.1% of gentamicin sulfate (Cultilab).

2.5. Cell viability assessment of L. amazonensis

Determine whether Amph-B maintains its antileishmanicidal properties after γ irradiation, increasing concentrations of I/Amph-B were evaluated. Promastigote forms of L. *amazonensis* pH8 were cultivated without Amph-B as a negative treatment control. About 200 parasites were cultivated under three Amph-B concentrations: 16.7 nM (1), 25.1 nM (2), and 33.4 nM (3), to establish a positive control. The percentage of growth inhibitión was calculated according to Eq. (1), using L. *amazonensis* pH8 culture without treatment as a negative control (Sunil et al., 2017).

$$\text{Growth Inhibition } (\%) = \frac{(O.D._{\ Control} \ - - \ O.D._{Treatment})}{O.D._{\ Control}} \times 100 \quad (1)$$

The same Amph-B(1–3) concentrations were incorporated into the hydrogel and irradiated by γ irradiation. As a negative control for parasite growth, the same hydrogel mass was used without Amph-B respecting the same ratio of medium added. Different quantities of hydrogel with and without Amph-B (0.883, 1.324, and 1.7 g/mL) were added to pH8 strain at 5 × 10^6 promastigotes in the early stationary phase (day 4) to a final volume of 0.5, 1.0, and 1.5 mL of M199 medium respectively. The plates, with parasites and hydrogel, were incubated at

24 °C for 24 or 48 h. After each period, the promastigotes were centrifuged at 1300 g for 10 mins, re-suspended in 5 mM PBS-glucose, and transferred to fresh culture plates. Cell viability was assessed by the addition of MTT (3-[4.5-*dimethyl*-2-*thiazolyl*]−2.5-diphenyl-2H-tetrazolium bromide). After a 50 min incubation at 24 °C, 10% SDS was added and optical density (O.D.) was read at 595 nm (Cicenia et al., 2015).

The quantity of promastigotes of the pH8 strain, prior to exposure to the different treatments, was established at an average concentration of 2 × 103 promastigotes per culture, the above mentioned concentration was quantified by flow cytometry in a Guava® easyCyte equipment (Merck Millipore). A culture at the same initial concentration, but without any treatment, was used as a negative control group. The percentage growth inhibition of the promastigotes population was determined by Eq. (1), in which the O.D. the parameter was changed to the number of cells quantified by flow cytometry.

2.6. Amph-B structure theoretical simulation

Molecular modeling was performed with the GaussView program. All calculations were carried out in GAUSSIAN 09, using the functional B3Lyp (Lee et al., 1988). All atoms were represented by a 6–31G(d) basis set (Hehre and Lathan, 1972). The energies were calculated in the gas phase until they reached their optimized structure at 298.15 K.

3. Results and discussion

3.1. Stability of Amph-B

Amph-B is not soluble in water but is soluble in excipients such as sodium deoxycholate, sodium hydroxide, and citric acid. Sodium deoxycholate is supplied with commercially available Amph-B (Silva et al., 2013; Hussain et al., 2016). After solubilization in this excipient, Amph-B is completely miscible as an aqueous solution and coexists as a mixture of soluble monomers, oligomers, and insoluble aggregates (Torrado et al., 2008; Ernst et al., 1981). Using UV–Vis spectroscopy we determined the molecular aggregation states of Amph-B. The different aggregation states within the same formulation depend on factors such as temperature, concentration, and dispersion forces. Amph-B was exposed to 15 kGy γ irradiation at 25 °C and both Amph-B and I/Amph-B samples were subjected to UV–Vis. According to the literature, at concentrations lower than 0.1 mgmL^{-1} Amph-B is typically present in its monomeric form characterized by three peaks: one peak between 406 and 409 nm in both absorption and circular dichroism spectra and the other two peaks at 363 and 383 nm (Bolard et al., 1980) The presence of three clear peaks on the same curve is characteristic of its monomeric

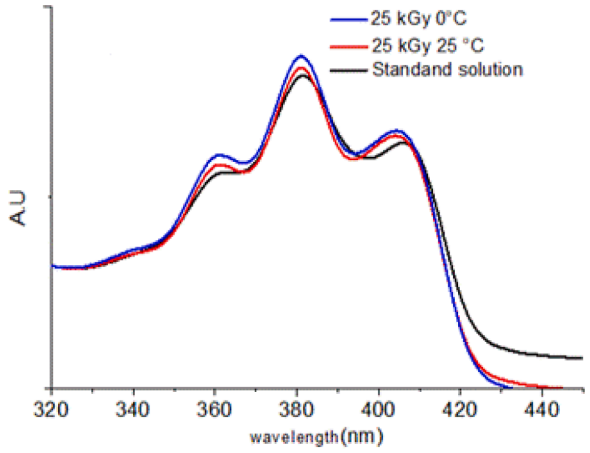

Fig. 1. UV-Visible Amax Amph-B solution (non irradiated) and irradiated I/Amph-B solution at 15-kGy dose and at the temperatures of 0 °C and 25 °C temperature.

form, in both irradiated and non-irradiated samples (Fig. 1). Furthermore, different temperatures (0 °C or 25 °C) exerted on I/Amph-B did not alter the intensity of the three peaks when compared with Amph-B. These findings confirm that during γ irradiation different temperatures do not alter the monomeric nature of Amph-B.

To further investigate the stability of the Amph-B structure when exposed to γ irradiation, we employed the use of the HPLC-MS hyphenated technique. Characterization of Amph-B was analyzed using a fragmentation profile (Fig. 2a) which identified the most abundant precursor ion produced as $(M + Na)^+$ and a mass/charge (m/z) ratio of 946.56 (Fig. 2b), and a product ion of m/z 906.56 (Fig. 2c). MS parameters were optimized to achieve selectivity and sensitivity in the electrospray mode ESI$^+$by analysis of the base peak chromatogram (BPC) which describes peak intensity using time-dependent scanning (Al-Quadeib et al., 2014).

Amph-B chromatogram shows an association of the drug to sodium deoxycholate, at 3.5 min and after 10 min (Fig. 3a), which is in accord with prior publication. Free and liposome compartmentalization of Amph-B in human plasma was determined by LC/MS following solid-phase extraction and protein precipitation techniques (Deshpande et al., 2010; Rodrigues and Khalil, 2014) The molecular ions for Amph-B were m/z 924 (monoisotopic without vehicle) and the product ion to m/z 906. A similar modified method was used by Hong et al. for the determination of free Amph-B from ultrafiltrate (Hong et al., 2007). The transition of masses to m/z 906.56 was observed and is specific for Amph-B (Fig. 3b). The precursor ion formed was $(M + Na)^+$ with an m/z 946.56 shows sodium adduct formation and the most abundant fragment ion as $(M - OH)^+$ of m/z 906.56. The fragment refers to the loss of 17 mass units (Krause et al., 1982), which suggests the loss of a hydroxyl (OH^-) group. The formation of the sodium adduct is justified by higher vehicle concentrations compared to the previous solubilized drug formulation.

The same observations were confirmed using chromatography and in the fragmentation profile analyses of I/Amph-B samples irradiated at 15 kGy at 25 °C (Fig. 3c, d). The fragmentation profile suggests that I/Amph-B did not suffer fragment loss due to γ irradiation, as the presence of molecular ion m/z 906.56 did not show changes in their structure and had a similar time retention when compared to the non-irradiated Amph-B sample. This result shows that gamma irradiation does not modify the molecular mass of Amph-B,

Vasil'eva et al. reported that γ irradiation of Amph-B in a dose range between 10 and 300 kGy induced a dose-dependent degradation of its polyene fragment (Vasil'eva et al., 1975). In our studies, the effect of 15 kGy γ irradiation on Amph-B does not generate relevant structural modifications. Furthermore, polyene-related signals of Amph-B detected by 1H NMR spectrum were between 6 and 6.5 ppm and showed no noticeable structural differences (Fig. 4). Based on these findings, any small changes in structure as a result of 15 kGy should not affect its antimicrobial activity because Amph-B binds to ergosterol, the sterol component of fungal cell membranes, leading to alterations in cell permeability, which in turn promote cell leakage and subsequent cell death (Robinson and Nahata, 1999). We show that 15 kGy was not enough to degrade the polyene fragment (Fig. 4a).

Using the 1H NMR spectrum simulated by DFT (Fig. 5) it was possible to analyze the experimental spectrum.. The signals generated after irradiation at 2.67 ppm (dd, 1H), 3.1 ppm (t, 1H), 3.84 ppm (d, 1H), and 3.96 ppm (3H) (Fig. 4b), appear to be rearrangements of the OH^- groups due to changes between intermolecular interactions. Amph-B's antibiotic activity is reduced when exposed to higher (50 kGy) irradiation doses, as reported by Fleurette et al. (Fleurette et al., 1975).

3.2. Gamma irradiation of Hydg/Amph-B

The physical properties of hydrogels are malleability, softness, and transparency (Fig. 6). Cobalt-60 ionizing radiation was used to crosslink the aqueous polymer solutions to create a solid, sterilized hydrogel. The

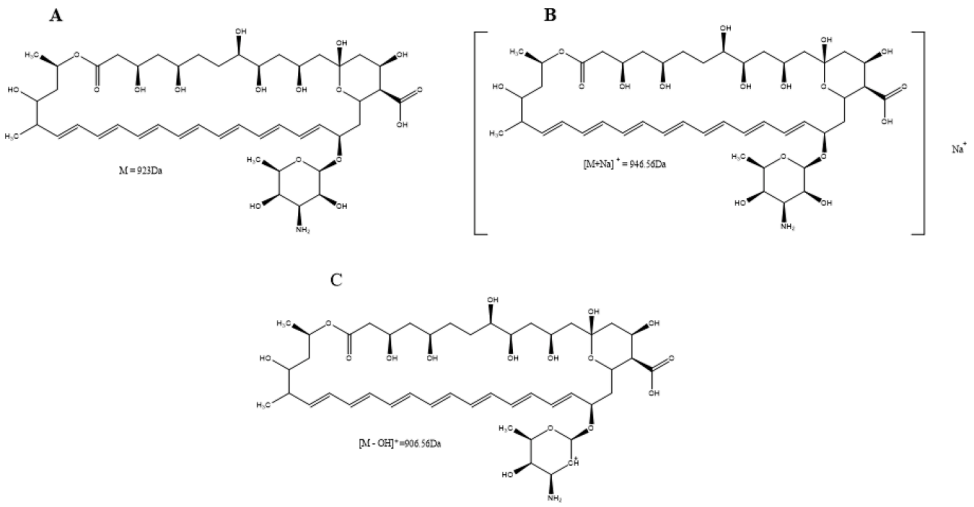

Fig. 2. . A) Amph-B structure, B) sodium adduct formation and C) precursor ion and the ion in m / z 906.56 Da.

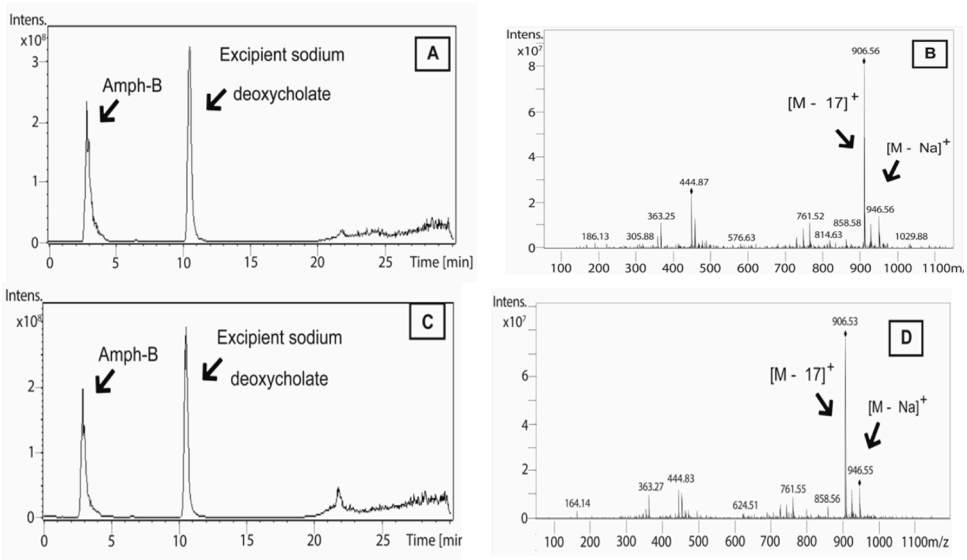

Fig. 3. (A and B) The non-irradiated Amph-B standard, (C and D) Amph-B irradiated at 25 °C temperature and 15 kGy doses obtained by chromatography followed by mass.

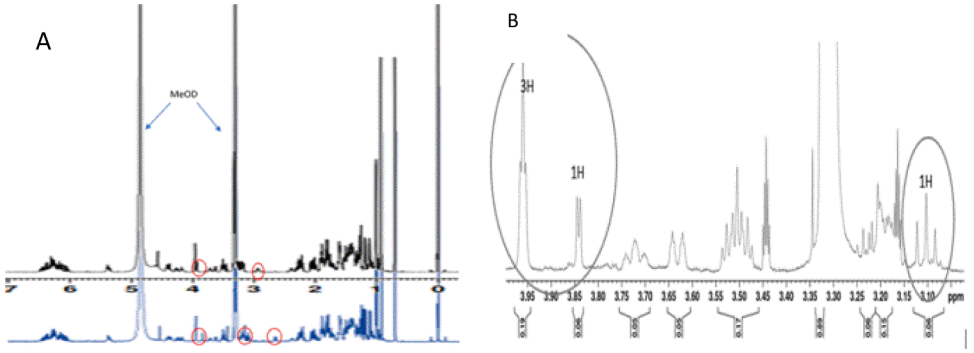

Fig. 4. 1H NMR (500 MHz, ppm). A) In black, before irradiation and in blue after irradiation spectra. The red circles show the signals that change. B) Detail of the spectra. (For interpretation of the references to colour in this figure legend, the reader is referred to the web version of this article.)

advantage of using ionizing radiation, aside from its ability to simultaneously crosslink and sterilize, is that it does not require the addition of chemical additives or cross-linkers which can lead to the generation of by-products (Sasaki et al., 2018; Zhu et al., 2016).

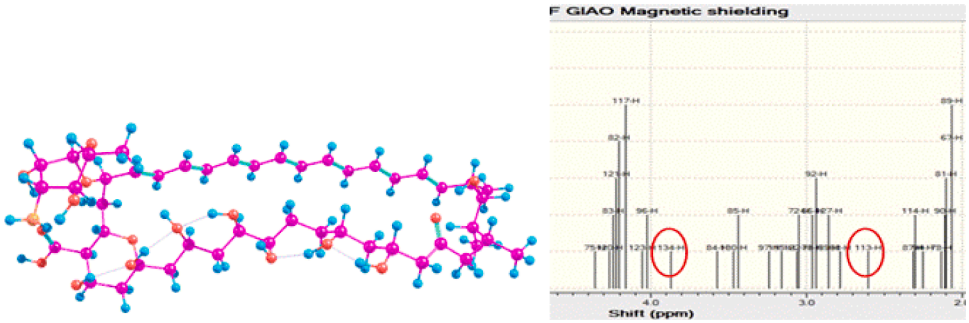

Fig. 5. Simulated geometry and RMN spectra for Amph-B after optimization, the red circles show the signals that were related to the experimental NMR signals. (For interpretation of the references to colour in this figure legend, the reader is referred to the web version of this article.)

Fig. 6. Hydg/Amph-B after radiation process results in malleable, soft and transparent hydrogel.

3.3. Extraction of Amph-B from the hydrogel

The UV–Vis absorption spectrum of Amph-B after it is released from the hydrogel allows for a qualitative analysis of both its release ability and its drug stability after exposure to γ irradiation (Fig. 7). Interestingly, Fig. 7 illustrates the cumulative Amax peaks at different time intervals of Amph-B. We identified that the hydrogel starts to release the drug in the first hour and is maintained for almost 12 h. Interestingly, the three peaks identified in Fig. 1 (412 nm, 389 nm, and 365 nm) are also conserved under what conditions (Fig. 7), indicating that the drug is stable after exposure to 15 kGy γ irradiation in the polymer solution. Based on our findings we assume that the activity of the drug remained after irradiation in the hydrogel.

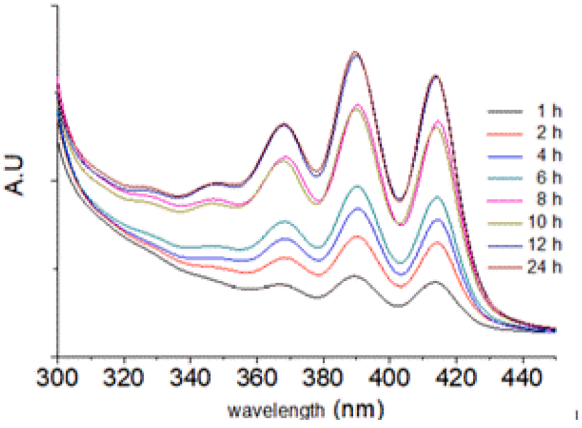

Fig. 7. The cumulative Amax peaks at different times intervals of the Amph-B incorporated into the irradiated hydrogel matrix at 15 kGy dose and at 25 °C.

3.4. Cell viability

Flow cytometry allowed determining an inhibitory concentration of 50% of the population of promastigotes (IC_{50}) within the first 24 h of exposure to the conditions of the Amph – B1 treatment, which corresponded to an IC_{50} = 16.7 nM of Amph –B (Fig. 8). The $_{IC50/Amph\text{-}B1}$ value obtained here is comparatively lower than others reported in the literature (Table. 1). The results show that at this same concentration of 16.7 nM, up to 99% of the promastigote population was inhibited at 48 h. The value obtained from $IC50_{/Amph\text{-}B1}$ mentioned above is highly relevant because the cell doubling time of promastigotes is around 6 to 7 h under *in vitro* conditions (Wheeler et al., 2011; Coelho et al., 2008), therefore, we present a new possible therapeutic window, whose action falls within the first 24 h, where it would be possible to limit the growth of the parasitic population in the promastigote stage. However, as shown in Table (2), after 48 h it is not possible to ensure that the parasitic life cycle has been completely limited. Despite this, the $IC_{50/Amph\text{-}B1}$ value obtained, represents a good therapeutic approximation given that in the clinic there is not an optimal dose - time relationship for the treatment of leishmaniasis. In subsequent studies in which longer exposure times are

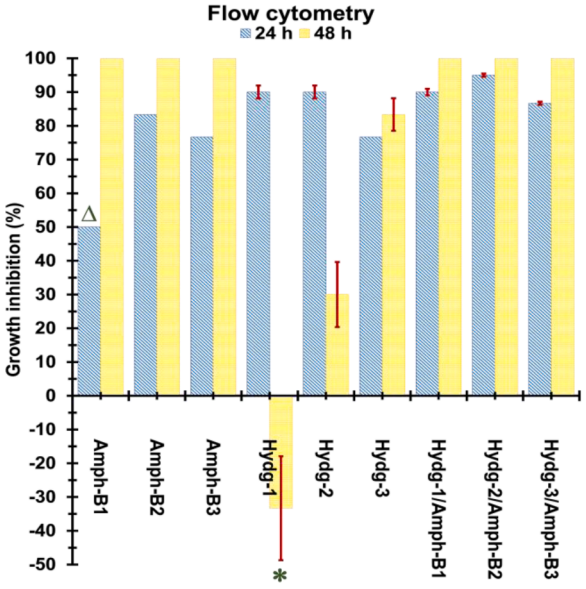

Fig. 8. Inhibition of population *in vitro* of L. *amazonensis* promastigotes. (Δ) indicates the treatment with an IC50 = 16.7 nM at 24 h of exposure. (*) indicates the increase in the promastigote population (Treatment> Control). The error bars correspond to the SE of the triplicate per test.

Table 1
IC_{50} values of Amph-B against L. *amazonensis*.

	Year	IC_{50}	
		(nM)	L/E
Experimental	*2020*	*16.7*	—
Chávez - Fumagalli,M.A. et al. (Buenger et al., 2012)	2015	129.86	7.78
Braga,F.G. et a. (Demeter et al., 2017)	2014	973.9	58.32
Ruiz, H. et al. (Aqil et al., 2005)	2007	248.90	14.90

L/*E*=IC_{50} value in literature in relation to the experimental value obtained.

considered, it will be possible to verify whether the effect of said IC50 / Amph-B1 is really a cytotoxic or cytostasis-like effect on the promastigote population (Mensa-Wilmot et al., 1999; Anttila et al., 2019; Freshney, 2016; Galluzzi et al., 2009; Kroemer et al., 2005).

On the other hand, it was observed that the treatment with Hydg-1 at 48 h gave negative values regarding the inhibition of the population (Table. 2). This means that the population of promastigotes under Hydg-1 treatment was greater than the control population, indicating that at least at 48 h 10% of promastigotes that were not previously inhibited or trapped by the composition and/or structure of Hydg-1, not only did it survive, but the microenvironmental conditions established by Hydg-1 allowed an increase of the population close to 33% compared to the initial population. In contrast, the combination Hydg-1/Amph-B1, managed to counteract this phenomenon, reaching inhibition values of the population close to 100% at 48 h, as with the Amph-B1 treatment.

Likewise, the Amph-B2 treatment showed an inhibition capacity at 24 h of around 83.33%, this being the maximum value determined in this study for the exposure of promastigotes to the drug, which was able to achieve an approximate inhibition of the 100% at 48 h. Similarly, when testing the Hydg-2/Amph-B2 combination, the best results were obtained both at 24 and 48 h of exposure with 95.0 and 100%, respectively. On the other hand, the Hydg-3/Amph-B3 treatment, which contains the highest dose of Amph-B tested in this study, did not show good short-term results, possibly due to the fact that, as we have previously reported, the composition of this type of hydrogel affects both the swelling capacity and the drug release capacity, the efficiency in the release and action of this high concentration of Amph-B3 on the promastigote population being affected (Oliveira et al., 2016).

Table 2
Inhibition of population growth and metabolic activity of L. amazonensis promastigotes *in vitro*.

Treatments	Growth (%)		Metabolic (%)	
	24 h	48 h	24 h	48 h
Amph-B1 (16.7 nM)	***50.00***	***99.97***	***97.50***	***94.87***
Amph-B2 (25.1 nM)	83.33	99.97	97.50	94.87
Amph-B3 (33.4 nM)	76.67	99.97	97.50	96.15 (7.4)
Hydg-1 (0.883 g/ mL)	***90.00 (1.9)***	***−33.33 (15.4)******	***85.00 (1.4)***	***−7.69[a] (4.4)***
Hydg-2 (1.324 g/ mL)	90.00 (1.9)	30.00 (9.6)	60.00 (1.4)	7.69 (4.4)
Hydg-3 (1.7 g/mL)	76.67	83.33 (4.8)	56.25 (5.8)	79.49
Hydg-1/Amph-B1	90.00 (1.0)	99.97	97.50	96.15
Hydg-2/Amph-B2	***95.00 (0.5)***	***99.97***	***97.50***	***96.15***
Hydg-3/Amph-B3	86.67 (0.5)	99.97	97.50	96.15

+The data were calculated with Eq. (1) considering PH8 without treatment as control.
++Values in parentheses correspond to the standard error of a series of triplicates.
+++The negative sign corresponds to a behavior where the value Treatment> Control.

3.5. Metabolic activity

Through the MTT test, the action of Amph-B on the metabolic activity in the promastigote population was analyzed (Fig. 9), obtaining results consistent with those previously mentioned, that is, for the case of the Hydg-1 treatment, found a decrease or inhibition in metabolic activity of up to 85%, we assume that the missing 15% would correspond to the metabolic activity developed by the 10% of the surviving population in this treatment, even an increase in activity was observed at 48 h. This change was due to the fact that the population of promastigotes under treatment was greater than the control population (Fig. 9§), however, this increase in metabolic activity was not in line with the increase in the population of promastigotes as might be expected, it is worth mentioning that this type of disparity between population and metabolic activity is not entirely strange as mentioned by Freshney, R.I. (2016). However, we could suggest that this behavior, product of the 10% of the surviving population responsible for the new population, together present a decrease in their metabolic activity that would allow the new promastigotes to maintain a minimal survival function, possibly establishing a population resistant to Amph-B, the latter will have to be verified later by molecular techniques.

Likewise, it was observed that the treatments that included Amph-B alone or in combination with some Hydg, showed inhibition of metabolic activity close to 97% at 24 h, but only the combination Hydg-2/Amph-B2 maintained a value maximum inhibitory at 48 h after exposure (Table. 2). This combination is ideal to be evaluated in other models such as co-cultures and skin injury in small species. In any case, we have demonstrated from the biological point of view that obtaining the hydrogel proposed here by radiation has no effect on the antiparasitic activity of amph-B and in particular for the case against promastigotes under *in vitro* culture conditions.

4. Conclusion

The stability of Amph-B was qualified by the UV–Vis technique, RMN, and HPL-MS which confirmed its spectroscopic behavior as monomeric. The presence of Amph-B could be characterized by three absorption wavelength bands: 363, 383, and 406 nm by NMR. The polyene-related signals of the antibiotic ranged from 6 to 6.5 ppm and

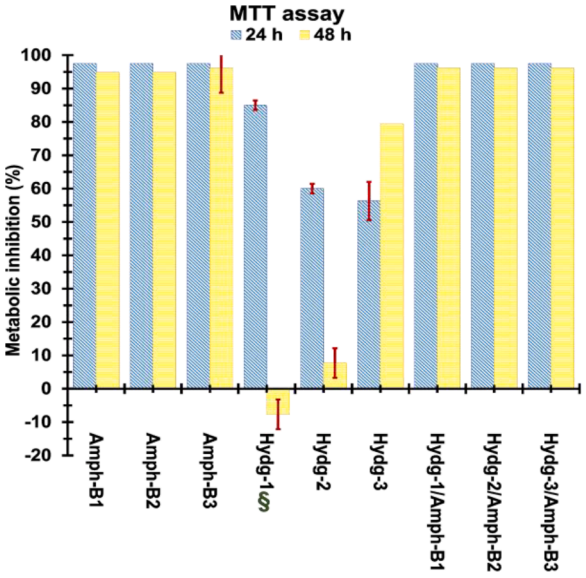

Fig. 9. Inhibition of mitochondrial metabolic activity in L. amazonensis promastigotes. (§) shows an increase in metabolic activity related to the increase in the promastigote population. The error bars correspond to the SE of the triplicate per test.

showed no noticeable change. A fragmentation profile using HPLC-MS analytical technique was generated specific to Amph-B of *m/z* 946.56 to 906.56. Importantly, no chromatographic signs of product decomposition were observed. The irradiation dose of 15 kGy was sufficient for crosslinking and sterilization at either 0 °C or 25 °C, and we confirmed temperature did not play a critical role in modifying the structure of Amph-B. It could be hypothesized that Amph-B may have evaded degradation during irradiation by being encapsulated in the polymeric matrix and therefore protected. Amph-B activity was measured by its ability to inhibit the growth of L. *amazonensis* promastigotes. We did not observe differences between the leishmanicidal activity of I/Amph-B or Amph-B. Hence, we demonstrate that hydrogels which undergo sterilization and cross-linking by ionizing radiation are potentially safe to be administered as aseptic material. Finally, given the promising results obtained, in our working group we have considered to carry out subsequent studies in co-cultivation with macrophages and a model of injured skin in small species, which will allow us to evaluate the biosecurity of this proposal as a viable alternative for its application in preclinical tests in humans. Therefore, Amph-B incorporated into the hydrogel matrix is a fully viable and alternative treatment option for lesions of cutaneous Leishmaniasis.

CRediT authorship contribution statement

Maria José Alves de Oliveira: Conceptualization, Methodology, Validation, Formal analysis, Investigation, Writing - original draft, Writing - review & editing, Project administration. **Gethzemani Mayeli Estrada Villegas:** Conceptualization, Writing - review & editing. **Flávia Daniela Motta:** Formal analysis. **Omar Fabela-Sánchez:** Conceptualization, Software, Validation, Data curation, Writing - review & editing. **Arián Espinosa-Roa:** Conceptualization, Software, Data curation, Writing - review & editing. **Wesley Luzetti Fotoran:** Methodology, Validation, Formal analysis. **Janaína Capelli Peixoto:** Methodology, Validation, Formal analysis. **Fabia Tomie Tano:** Formal analysis. **Ademar Benévolo Lugão:** Resources. **Pablo Antonio Salvador Vásquez:** Methodology, Resources, Writing - review & editing, Project administration.

Declaration of Competing Interest

The authors confirm that there are no conflicts of interest.

Acknowledgments

We are grateful for financial support by the National Nuclear Energy Commission (CNEN). We also thank M.*Sc* Paulo S. Santos from (CETR-IPEN-SP) for irradiation support.

Supplementary materials

Supplementary material associated with this article can be found, in the online version, at doi:10.1016/j.actatropica.2020.105805.

References

Abad, L.V., 2016. Radiation Processing of Natural Polymers For Medical and Healthcare Applications Chapter 10. International Atomic Energy Agency (IAEA): IAEA.

Al-Mohammed, H.I., Chance, M.L., Bates, P.A., 2005. Production and Characterization of Stable Amphotericin-Resistant Amastigotes and Promastigotes of Leishmania mexicana. Antimicrob. Agents Chemother. 49 (8), 3274–3280. https://doi.org/10.1128/aac.49.8.3274-3280.2005.

Al-Quadeib, B.T., Radwan, M.A., Siller, L., Mutch, E., Horrocks, B., Wright, M., Alshaer, A., 2014. Therapeutic monitoring of amphotericin B in Saudi ICU patients using UPLC MS/MS assay. Biomed. Chromatogr.: BMC 28 (12), 1652–1659. https://doi.org/10.1002/bmc.3198.

Amato, V.S., Tuon, F.F., Siqueira, A.M., Nicodemo, A.C., Neto, V.A., 2007. Treatment of mucosal leishmaniasis in Latin America: systematic review. Am. J. Trop. Med. Hyg. 77 (2), 266–274.

Anttila, J.V., Shubin, M., Cairns, J., Borse, F., Guo, Q., Mononen, T., Vázquez-García, I., Pulkkinen, O., Mustonen, V., 2019. Contrasting the impact of cytotoxic and cytostatic drug therapies on tumour progression. PLoS Comput. Biol. 15 (11), e1007493 https://doi.org/10.1371/journal.pcbi.1007493.

Aqil, M., Zafar, S., Ali, A., Ahmad, S., 2005. Transdermal Drug Delivery of Labetolol Hydrochloride: system Development, In Vitro; Ex Vivo and In Vivo Characterization. Curr. Drug Deliv. 2 (2), 125–131. https://doi.org/10.2174/1567201053586038.

Bhattarai, N., Gunn, J., Zhang, M., 2010. Chitosan-based hydrogels for controlled, localized drug delivery. Adv. Drug Deliv. Rev. 62 (1), 83–99. https://doi.org/10.1016/j.addr.2009.07.019.

Bolard, J., Seigneuret, M., Boudet, G., 1980. Interaction between phospholipid bilayer membranes and the polyene antibiotic amphotericin B: lipid state and cholesterol content dependence. Biochim. Biophys. Acta 599 (1), 280–293. https://doi.org/10.1016/0005-2736(80)90074-7.

Borborema, S.E., Junior, H.F., Junior, J.A., Nascimento, N.D., 2005. In Vitro antileishmanial properties of neutron-irradiated meglumine antimoniate. Brazilian Arch. Biol. Technol. 48 (Spe2), 63–68. https://doi.org/10.1590/s1516-89132005000700009.

Buenger, D., Topuz, F., Groll, J., 2012. Hydrogels in sensing applications. Prog. Polym. Sci. 37 (12), 1678–1719. https://doi.org/10.1016/j.progpolymsci.2012.09.001.

Chávez-Fumagalli, M.A., Ribeiro, T.G., Castilho, R.O., Fernandes, S.O., Cardoso, V.N., Coelho, C.S., ..., Coelho, E.A., 2015. New delivery systems for amphotericin B applied to the improvement of leishmaniasis treatment. Rev. Soc. Bras. Med. Trop. 48 (3), 235–242. https://doi.org/10.1590/0037-8682-0138-2015.

Cicenia, A., Santagelo, F., Gambardella, L., Iebba, V., Scirocco, A., Pallotta, L., Marignani, M., Chirletti, P., Carabotti, M., Schippa, S., Corazziari, E., Severi, C., 2015. Op-3 the Protective Role of Lactobacillus Rhamnosus Gg-Derived Factors against Lps-Induced Damage of Human Colonic Smooth Muscle Cells. J. Pediatr. Gastroenterol. Nutr. 61 (4), 509–510. https://doi.org/10.1097/01.mpg.0000472207.54141.fa.

Coelho, A.C., Gentil, L.G., da Silveira, J.F., Cotrim, P.C., 2008. Characterization of Leishmania (Leishmania) amazonensis promastigotes resistant to pentamidine. Exp. Parasitol. 120 (1), 98–102. https://doi.org/10.1016/j.exppara.2008.03.018.

Dash, M., Chiellini, F., Ottenbrite, R., Chiellini, E., 2011. Chitosan—A versatile semi-synthetic polymer in biomedical applications. Prog. Polym. Sci. 36 (8), 981–1014. https://doi.org/10.1016/j.progpolymsci.2011.02.001.

Demeter, M., Virgolici, M., Vancea, C., Scarisoreanu, A., Kaya, M.G., Meltzer, V., 2017. Network structure studies on γ–irradiated collagen–PVP superabsorbent hydrogels. Radiat. Phys. Chem. 131, 51–59. https://doi.org/10.1016/j.radphyschem.2016.09.029.

Deshpande, N.M., Gangrade, M.G., Kekare, M.B., Vaidya, V.V., 2010. Determination of free and liposomal amphotericin B in human plasma by liquid chromatography-mass spectroscopy with solid phase extraction and protein precipitation techniques. J. Chromatogr. B Analyt. Technol. Biomed. Life Sci. 878 (3–4), 315–326. https://doi.org/10.1016/j.jchromb.2009.11.036.

Ernst, C., Grange, J., Rinnert, H., Dupont, G., Lematre, J., 1981. Structure of amphotericin B aggregates as revealed by UV and CD spectroscopies. Biopolymers 20, 1575–1588. https://doi.org/10.1002/bip.1981.360200802.

Fleurette, J., Madier, S., Transy, M.J., 1975. Bacteriostatic Activity of Various Antibiotics After Gamma-Ray irradiation. Activite bacteriostatique De Differents Antibiotiques Apres Irradiation Par Rayons Gamma. International Atomic Energy Agency (IAEA): IAEA.

Freshney, R.I., 2016. Culture of Animal Cells: A Manual of Basic Technique and Specialized Applications: Seventh Edition, 7th ed. Wiley-Blackwell.

Galluzzi, L., Aaronson, S.A., Abrams, J., Alnemri, E.S., Andrews, D.W., Baehrecke, E.H., Bazan, N.G., Blagosklonny, M.V., Blomgren, K., Borner, C., Bredesen, D.E., Brenner, C., Castedo, M., Cidlowski, J.A., Ciechanover, A., Cohen, G.M., De Laurenzi, V., De Maria, R., Deshmukh, M., Dynlacht, B.D., ..., Kroemer, G., 2009. Guidelines for the use and interpretation of assays for monitoring cell death in higher eukaryotes. Cell Death Differ. 16 (8), 1093–1107. https://doi.org/10.1038/cdd.2009.44.

Hehre, W.J., Lathan, W.A., 1972. Self-consistent molecular orbital methods. XIV. an extended gaussian-type basis for molecular orbital studies of organic molecules. inclusion of second row elements. J. Chem. Phys. 56 (11), 5255–5257. https://doi.org/10.1063/1.1677028.

Henke, A., Kadlubowski, S., Ulanski, P., Rosiak, J.M., Arndt, K., 2005. Radiation-induced cross-linking of polyvinylpyrrolidone-poly(acrylic acid) complexes. Nuclear Instrum. Methods Phys. Res. Section B: Beam Interact. Mater. Atoms 236 (1–4), 391–398. https://doi.org/10.1016/j.nimb.2005.04.003.

Holback, H., Yeo, Y., Park, K., 2011. 1 - Hydrogel swelling behavior and its biomedical applications. In: Rimmer, S. (Ed.), Biomedical Hydrogels. Woodhead Publishing, pp. 3–24. https://doi.org/10.1533/9780857091383.1.3.

Hong, Y., Shaw, P.J., Tattam, B.N., Nath, C.E., Earl, J.W., Stephen, K.R., McLachlan, A.J., 2007. Plasma protein distribution and its impact on pharmacokinetics of liposomal amphotericin B in paediatric patients with malignant diseases. Eur. J. Clin. Pharmacol. 63 (2), 165–172. https://doi.org/10.1007/s00228-006-0240-x.

Hussain, A., Singh, V.K., Singh, O.P., Shafaat, K., Kumar, S., Ahmad, F.J., 2016. Formulation and optimization of nanoemulsion using antifungal lipid and surfactant for accentuated topical delivery of Amphotericin B. Drug Deliv. 23 (8), 3101–3110. https://doi.org/10.3109/10717544.2016.1153747.

Khampieng, T., Brikshavana, P., Supaphol, P., 2014. Silver nanoparticle-embedded poly (vinyl pyrrolidone) hydrogel dressing: gamma-ray synthesis and biological evaluation. J. Biomater. Sci. Polym. Ed. 25 (8), 826–842. https://doi.org/10.1080/09205063.2014.910154.

Krause, P.J., Owens, N.J., Nightingale, C.H., Klimek, J.J., Lehmann, W.B., Quintiliani, R., 1982. Penetration of amoxicillin, cefaclor, erythromycin-sulfisoxazole, and

trimethoprim-sulfamethoxazole into the middle ear fluid of patients with chronic serous otitis media. J. Infectious Dis. 145 (6), 815–821. https://doi.org/10.1093/infdis/145.6.815.

Kroemer, G., El-Deiry, W.S., Golstein, P., Peter, M.E., Vaux, D., Vandenabeele, P., Zhivotovsky, B., Blagosklonny, M.V., Malorni, W., Knight, R.A., Piacentini, M., Nagata, S., Melino, G., 2005. & Nomenclature committee on cell death. classification of cell death: recommendations of the nomenclature committee on cell death. Cell Death Differ. 12 (Suppl 2), 1463–1467. https://doi.org/10.1038/sj.cdd.4401724.

Lee, C., Yang, W., Parr, R.G., 1988. Development of the Colle-Salvetti correlation-energy formula into a functional of the electron density. Phys. Rev., B Condens. Matter 37 (2), 785–789. https://doi.org/10.1103/physrevb.37.785.

Lee, J.W., Petersen, M.E., Lin, P., Dressler, D., Bekersky, I., 2001. Quantitation of free and total amphotericin B in human biologic matrices by a liquid chromatography tandem mass spectrometric method. Ther. Drug Monit. 23 (3), 268–276. https://doi.org/10.1097/00007691-200106000-00015.

Mensa-Wilmot, K., Garg, N., McGwire, B.S., Lu, H.G., Zhong, L., Armah, D.A., LeBowitz, J.H., Chang, K.P., 1999. Roles of free GPIs in amastigotes of Leishmania. Mol. Biochem. Parasitol. 99 (1), 103–116. https://doi.org/10.1016/s0166-6851(99)00003-1.

Murphy, B., Anderson, K., Borissow, C., Caffrey, P., Griffith, G., Hearn, J., ..., Rawlings, B., 2010. Isolation and characterisation of amphotericin B analogues and truncated polyketide intermediates produced by genetic engineering of Streptomyces nodosus. Org. Biomol. Chem. 8 (16), 3758. https://doi.org/10.1039/b922074g.

Oliveira, M.J.A., Maia, R., Braz, L.A., Lugao, A.B., Amato, V.S., 2016. Topical treatment of cutaneous leishmaniasis: wound reduction in mice using n-methyl glucamine from PVP and nano clay membranes. J. Dermatol. Res. Therapy 2 (5). https://doi.org/10.23937/2469-5750/1510036.

Robinson, R.F., Nahata, M.C., 1999. A comparative review of conventional and lipid formulations of amphotericin B. J. Clin. Pharm. Ther. 24 (4), 249–257. https://doi.org/10.1046/j.1365-2710.1999.00220.x.

Rodrigues, Caroline Danziato, Khalil, Najeh Maissar, 2014. Rubiana Mara Mainardes Determination of amphotericin B in PLA-PEG blend nanoparticles by HPLC-PDA Brazilian. J. Pharm. Sci. 50 (4) https://doi.org/10.1590/S1984-82502014000400021.

Ruiz, H.K., Serrano, D.R., Dea-Ayuela, M.A., Bilbao-Ramos, P.E., Bolás-Fernández, F., Torrado, J.J., Molero, G., 2014. New amphotericin B-gamma cyclodextrin formulation for topical use with synergistic activity against diverse fungal species and Leishmania spp. Int. J. Pharm. 473 (1–2), 148–157. https://doi.org/10.1016/j.ijpharm.2014.07.004.

Sasaki, S., Omata, S., Murakami, T., Nagasawa, N., Taguchi, M., Suzuki, A., 2018. Effect of gamma ray irradiation on friction property of poly(vinyl alcohol) cast-drying on freeze-thawed hybrid gel. Gels (Basel, Switzerland) 4 (2), 30. https://doi.org/10.3390/gels4020030.

Shu, C., Li, T., Yang, W., Li, D., Ji, S., Ding, L., 2018. Amphotericin B-conjugated polypeptide hydrogels as a novel innovative strategy for fungal infections. R. Soc. Open Sci. 5 (3), 171814 https://doi.org/10.1098/rsos.171814.

Silva, A.E., Barratt, G., Chéron, M., Egito, E.S., 2013. Development of oil-in-water microemulsions for the oral delivery of amphotericin B. Int. J. Pharm. 454 (2), 641–648. https://doi.org/10.1016/j.ijpharm.2013.05.044.

Soriano, I., Martín, A.Y., Évora, C., Sánchez, E., 2006. Biodegradable implantable fluconazole delivery rods designed for the treatment of fungal osteomyelitis: influence of gamma sterilization. J. Biomed. Mater. Res. Part A 77A (3), 632–638. https://doi.org/10.1002/jbm.a.30657.

Sosa, N., Pascale, J.M., Jiménez, A.I., Norwood, J.A., Kreishman-Detrick, M., Weina, P.J., ..., Grogl, M., 2019. Topical paromomycin for New World cutaneous leishmaniasis. PLoS Negl. Trop. Dis. 13 (5) https://doi.org/10.1371/journal.pntd.0007253.

Sumit Mishra, P.R., Sen, Gautam, Dey, Kartick Prasad, 2018. Preparation, Properties and Application of Hydrogels: A Review - Hydrogels. Springer, Singapore, pp. 145–173. https://doi.org/10.1007/978-981-10-6077-9_6 chapter 6.

Sunil, D., Kamath, R., Chandrashekhar, H., 2017. In Vitro Bioassay Techniques for Anticancer Drug Discovery and Development. CRC Press.

Tamargo, J., Heuzey, J.L., Mabo, P., 2015. Narrow therapeutic index drugs: a clinical pharmacological consideration to flecainide. Eur. J. Clin. Pharmacol. 71 (5), 549–567. https://doi.org/10.1007/s00228-015-1832-0.

Torrado, J.J., Espada, R., Ballesteros, M.P., Torrado-Santiago, S., 2008. Amphotericin B formulations and drug targeting. J. Pharm. Sci. 97 (7), 2405–2425. https://doi.org/10.1002/jps.21179.

Tutaj, K., Szlazak, R., Szalapata, K., Starzyk, J., Luchowski, R., Grudzinski, W., ..., Gruszecki, W.I., 2016. Amphotericin B-silver hybrid nanoparticles: synthesis, properties and antifungal activity. Nanomed.: Nanotechnol. Biol. Med. 12 (4), 1095–1103. https://doi.org/10.1016/j.nano.2015.12.378.

Vasil'eva, N.G., Dumova, A.M., Etingov, E.D., Bol'shakova, L.O., 1975. Vliianie gamma-oblucheniia na nekotorye biologicheskie i fiziko-khimicheskie svoĭstva polienovykh antibiotikov [Effect of gamma-irradiation on some biological and physico-chemical properties of polyene antibiotics. Antibiotiki 20 (11), 982–984.

Wheeler, R.J., Gluenz, E., Gull, K., 2011. The cell cycle of Leishmania: morphogenetic events and their implications for parasite biology. Mol. Microbiol. 79 (3), 647–662. https://doi.org/10.1111/j.1365-2958.2010.07479.x.

Wortmann, G., Pierson, J., Weintrob, A., Zapor, M., Magill, A., Ressner, R., ..., Hartzell, J., 2010. Lipsosomal Amphotericin B for Treatment of Cutaneous Leishmaniasis. Am. J. Trop. Med. Hyg. 83 (5), 1028–1033. https://doi.org/10.4269/ajtmh.2010.10-0171.

Yano, H., Hirayama, F., Kamada, M., Arima, H., Uekama, K., 2002. Colon-specific delivery of prednisolone-appended α-cyclodextrin conjugate: alleviation of systemic side effect after oral administration. J. Controlled Rel. 79 (1–3), 103–112. https://doi.org/10.1016/s0168-3659(01)00532-6.

Zhu, T., Teng, K., Shi, J., Chen, L., Xu, Z., 2016. A facile assembly of 3D robust double network graphene/polyacrylamide architectures via γ-ray irradiation. Compos. Sci. Technol. 123, 276–285. https://doi.org/10.1016/j.compscitech.2015.11.007.